



TITLE:

# Magnetocaloric effect of Sr-substituted BaFeO<sub>3</sub> in the liquid nitrogen and natural gas temperature regions

AUTHOR(S):

Yoshii, Kenji; Hayashi, Naoaki; Mizumaki, Masaichiro; Takano, Mikio

---

CITATION:

Yoshii, Kenji ...[et al]. Magnetocaloric effect of Sr-substituted BaFeO<sub>3</sub> in the liquid nitrogen and natural gas temperature regions. AIP Advances 2017, 7(4): 045117.

ISSUE DATE:

2017-04

URL:

<http://hdl.handle.net/2433/225279>

RIGHT:

© Author(s) 2017. All article content, except where otherwise noted, is licensed under a Creative Commons Attribution (CC BY) license (<http://creativecommons.org/licenses/by/4.0/>).

## Magnetocaloric effect of Sr-substituted BaFeO<sub>3</sub> in the liquid nitrogen and natural gas temperature regions

Kenji Yoshii, Naoaki Hayashi, Masaichiro Mizumaki, and Mikio Takano

Citation: *AIP Advances* **7**, 045117 (2017); doi: 10.1063/1.4982244

View online: <http://dx.doi.org/10.1063/1.4982244>

View Table of Contents: <http://aip.scitation.org/toc/adv/7/4>

Published by the *American Institute of Physics*

---

### Articles you may be interested in

[Magnetization reversal behavior and magnetocaloric effect in SmCr<sub>0.85</sub>Mn<sub>0.15</sub>O<sub>3</sub> chromites](#)

*Journal of Applied Physics* **121**, 043907 (2017); 10.1063/1.4974737

[Role of hydrogen carrier gas on the growth of few layer hexagonal boron nitrides by metal-organic chemical vapor deposition](#)

*AIP Advances* **7**, 045116 (2017); 10.1063/1.4982029

[Magnetic and nonmagnetic contributions to the heat capacity of metamagnetic shape memory alloy](#)

*Journal of Applied Physics* **121**, 183901 (2017); 10.1063/1.4983025

[Erbium diffusion in titanium dioxide](#)

*AIP Advances* **7**, 045202 (2017); 10.1063/1.4979923

[Topography evolution of germanium thin films synthesized by pulsed laser deposition](#)

*AIP Advances* **7**, 045115 (2017); 10.1063/1.4981800

[Study of magnetic ordering in the perovskite manganites Pr<sub>0.6</sub>Sr<sub>0.4</sub>Cr<sub>x</sub>Mn<sub>1-x</sub>O<sub>3</sub>](#)

*AIP Advances* **7**, 045302 (2017); 10.1063/1.4980019

---

# HAVE YOU HEARD?

Employers hiring scientists and  
engineers trust

**PHYSICS TODAY | JOBS**

[www.physicstoday.org/jobs](http://www.physicstoday.org/jobs)





## Magnetocaloric effect of Sr-substituted BaFeO<sub>3</sub> in the liquid nitrogen and natural gas temperature regions

Kenji Yoshii,<sup>1,a</sup> Naoaki Hayashi,<sup>2,b</sup> Masaichiro Mizumaki,<sup>3,4</sup>  
and Mikio Takano<sup>2,c</sup>

<sup>1</sup>Japan Atomic Energy Agency, Sayo, Hyogo 679-5148, Japan

<sup>2</sup>Institute for Integrated Cell-Material Sciences, Kyoto University, Kyoto 606-8501, Japan

<sup>3</sup>Japan Synchrotron Radiation Research Institute, Sayo, Hyogo 679-5198, Japan

<sup>4</sup>CREST, Japan Science and Technology Agency, 5 Sanbancho, Chiyoda-ku, Tokyo 102-0075, Japan

(Received 10 February 2017; accepted 12 April 2017; published online 20 April 2017)

We have investigated the magnetocaloric effect (MCE) of Ba<sub>1-x</sub>Sr<sub>x</sub>Fe<sup>4+</sup>O<sub>3</sub> ( $x \leq 0.2$ ), a series of cubic perovskites showing a field-induced transition from helical antiferromagnetism to ferromagnetism. The maximum magnetic entropy change ( $-\Delta S_{\max}$ ) at 50 kOe varies from  $\sim 5.8 \text{ J kg}^{-1} \text{ K}^{-1}$  ( $x=0$ ) to  $\sim 4.9 \text{ J kg}^{-1} \text{ K}^{-1}$  ( $x=0.2$ ), while the refrigerant capacity remains almost the same at  $\sim 165 \text{ J kg}^{-1}$ . Interestingly, the temperature of  $-\Delta S_{\max}$  decreases from  $\sim 116 \text{ K}$  to  $\sim 77 \text{ K}$  with increasing  $x$ , providing this series of rare-earth-free oxides with potential as a magnetic refrigerant for the liquefaction of nitrogen and natural gas. © 2017 Author(s). All article content, except where otherwise noted, is licensed under a Creative Commons Attribution (CC BY) license (<http://creativecommons.org/licenses/by/4.0/>). [<http://dx.doi.org/10.1063/1.4982244>]

Increasing demand for environmental protection has urged the development of refrigeration methods which are more efficient than the conventional gas compression-expansion cycle.<sup>1,2</sup> One of such methods is magnetic refrigeration based on the magnetocaloric effect (MCE) due to the magnetic entropy change caused by application of magnetic field ( $H$ ).<sup>1,2</sup> A considerably large MCE has been found in several systems such as Gd<sub>5</sub>(Si<sub>1-x</sub>Ge<sub>x</sub>)<sub>4</sub>,<sup>3</sup> MnAs,<sup>4</sup> La(Fe<sub>1-x</sub>Si<sub>x</sub>)<sub>13</sub>,<sup>5,6</sup> HoAgGa,<sup>7</sup> and perovskite-type Mn-oxides.<sup>8,9</sup> Generally, ferromagnets containing rare-earth elements with large atomic moments are advantageous because the field-induced entropy change near the Curie temperature is strongly enhanced.

Recently, we reported that a new perovskite, BaFeO<sub>3</sub>, is a candidate MCE material.<sup>10</sup> This oxide contains heavily oxidized Fe ions, Fe<sup>4+</sup> (3d<sup>4</sup>,  $S=2$ ), in the cubic perovskite structure ( $a \sim 3.97 \text{ Å}$ ).<sup>11</sup> The localized moments are ordered in an antiferromagnetic helical spin structure of the A-type (denoted as AHM) with the propagation vector oriented along the cubic axis,  $\mathbf{k} \parallel \langle 100 \rangle$ , below the Néel temperature of  $T_N \sim 111 \text{ K}$ , but application of a small field of  $H = 3 \text{ kOe}$  switches this complicated AHM spin structure to a simple ferromagnetic one (FM,  $3.5 \mu_B/\text{Fe}$ ).<sup>11</sup> A considerably large entropy change of  $\sim 5.8 \text{ J kg}^{-1} \text{ K}^{-1}$ , comparable to those of manganites, has been observed at  $\sim 116 \text{ K}$  at  $H = 50 \text{ kOe}$ , and the refrigerant capacity has been estimated to be  $\sim 172 \text{ J kg}^{-1}$ .<sup>10</sup> Interestingly, the magnetic and thermal hysteretic losses are negligibly small contrary to expectations that the Fe<sup>4+</sup>: $t_{2g}^3 e_g^1$  configuration with two-fold orbital degeneracy should bring about such losses caused by strong spin-lattice interactions. However, as revealed by photoelectron spectroscopic and X-ray absorption spectroscopic studies,<sup>12,13</sup> the real electronic configuration is close to Fe<sup>3+</sup> $\underline{L}$  (Fe<sup>3+</sup>:  $t_{2g}^3 e_g^2$ ,  $\underline{L}$ : ligand hole) in which the effect of orbital degeneracy is dispersed into the broad oxygen  $p$  hole band. It is also favorable that BaFeO<sub>3</sub> is rare-earth-free and stable against corrosion. This oxide may be suitable for the liquefaction of natural gas at  $\sim 110 \text{ K}$ <sup>14</sup> as well as cooling of cuprate superconductors.<sup>15</sup>

<sup>a</sup>E-mail: [yoshiike@spring8.or.jp](mailto:yoshiike@spring8.or.jp)

<sup>b</sup>Present address: Research Institute for Production Development, Kyoto 606-0805, Japan.

<sup>c</sup>Present address: Graduate School of Natural Science and Technology, Okayama University, Okayama 700-8530, Japan.



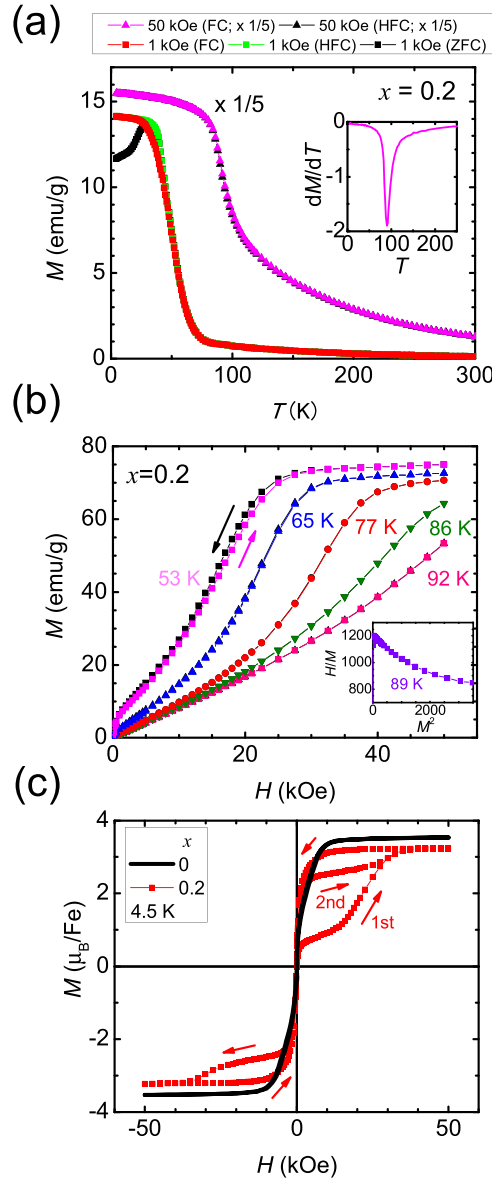


FIG. 1. (a) Magnetization-temperature ( $MT$ ) curves of  $\text{Ba}_{0.8}\text{Sr}_{0.2}\text{FeO}_3$  ( $x=0.2$ ). For an applied field ( $H$ ) of 1 kOe, the curves are shown for zero-field-cooling (ZFC), field-cooling (FC), and also heating after field-cooling (HFC). For  $H=50$  kOe, the curves are only shown for FC and HFC modes, since the ZFC curve was almost identical. The magnetization for this field was multiplied by 1/5. The inset shows the temperature derivative of the FC curve for  $H=50$  kOe. (b) Magnetization-magnetic field ( $MH$ ) curves for  $x=0.2$  at around the refrigeration temperature region. The data were measured in both increasing and decreasing in  $H$ , as shown for those at 53 K. The other curves were nearly identical in the two kinds of the measurement sequences. The inset shows the Arrott plot at a temperature near  $T_C$ , 89 K; its negative slope shows first-order nature of the magnetic transition. (c)  $MH$  curves at 4.5 K for  $x=0$  and 0.2. For  $x=0.2$ , both the 1st and 2nd curves are shown to demonstrate the hysteretic behavior.

The purpose of the present work is to investigate the MCE of the solid solution of  $\text{BaFeO}_3$  (BFO) and  $\text{SrFeO}_3$  (SFO),  $\text{Ba}_{1-x}\text{Sr}_x\text{FeO}_3$  (BSFO). SFO is also an antiferromagnetic cubic perovskite with a helical spin structure of the  $G$ -type with  $\mathbf{k} \parallel \langle 111 \rangle$  (denoted as GHM,  $T_N=134$  K), while the field-induced transition to ferromagnetism takes place at a very high field of  $\sim 400$  kOe.<sup>16</sup> As revealed recently,<sup>17</sup> the type of helical spin structure changes from  $A$  to  $G$  at  $x \geq 0.1$ . In comparison with the reversible field-induced AHM-FM transition, the GHM-FM transition is of the first order and is hysteretic. This makes the practical temperature- and field-dependence of magnetization complicated for  $x \geq 0.1$ , especially at low temperatures and low fields, but we have

believed that this solution system is worthy of being studied to clarify the chemical controllability of MCE.

Refrigeration below 77 K, mainly for the liquefaction of nitrogen, hydrogen and helium, is one of the two desired purposes of magnetic refrigeration, the other being operation at around room temperature.<sup>18</sup> Quite remarkably a rare-earth-free spinel system, Fe-doped  $\text{MnV}_2\text{O}_4$ , has very recently been found to show a large entropy change of  $\sim 5.8 \text{ J kg}^{-1} \text{ K}^{-1}$  at  $\sim 77 \text{ K}$ .<sup>19</sup> The performance of BSFO having lowered working temperatures will be described below.

The BSFO samples with  $x=0, 0.1$  and  $0.2$  were prepared as reported previously, i.e. by high temperature solid-state reactions and subsequent low temperature treatment with ozone for the final oxidation.<sup>17</sup> X-ray diffraction measurements showed that they were single-phase cubic perovskites ( $\text{Pm-3m}$ ).<sup>17</sup> The Sr substitution induced a shrinkage of the unit cell from  $a \sim 3.97 \text{ \AA}$  ( $x=0$ ) to  $\sim 3.94 \text{ \AA}$  ( $x=0.2$ ) because  $\text{Sr}^{2+}$  is smaller than  $\text{Ba}^{2+}$ . Magnetic measurements were carried out using a superconducting quantum interference device magnetometer (Quantum Design MPMS) below  $300 \text{ K}$  in a field range of  $H = \pm 50 \text{ kOe}$ .<sup>10</sup> Temperature ( $T$ )-dependence of magnetization ( $M$ ) was measured on heating after zero-field-cooling (ZFC), on field-cooling (FC), and also on heating after field-cooling (HFC). Magnetization-field ( $MH$ ) isotherm curves were measured in the protocol called the loop process noted later to avoid the thermal and magnetic histories.<sup>20</sup> The powder samples were pressed into a bar with a diameter of  $\sim 1 \text{ mm}$  and a height of  $\sim 4\text{--}5 \text{ mm}$ ; considering this shape as a uniform magnetized cylinder, the demagnetizing factor is  $\gamma \sim 0.1$ .<sup>21</sup> The demagnetizing field  $\gamma M$  was assumed to be small ( $< \sim 50 \text{ Oe}$ ) by using the saturation magnetization of  $M \sim 75\text{--}79 \text{ emu/g}$  at low temperatures with  $H=50 \text{ kOe}$  (For example, see Figs. 1b and 1c) and the density of  $\sim 6.28 \text{ g/cm}^3$  (shown later). This field is fairly smaller than the applied fields used for the calculations of MCE ( $H > \sim 10 \text{ kOe}$ ). Hence, the correction of the demagnetizing field was not performed.

The magnetization of  $\text{Ba}_{0.8}\text{Sr}_{0.2}\text{FeO}_3$  ( $x=0.2$ ) shows such strong  $T$ - and  $H$ -dependences as typically shown in Fig. 1(a). The low-field magnetization at  $H = 1 \text{ kOe}$  quickly increases/decreases at  $\sim 70 \text{ K}$  on cooling/heating, and the ZFC, FC, and HFC curves more or less deviate from each other below  $\sim 50 \text{ K}$ , while such an irreversibility is not seen at  $H = 50 \text{ kOe}$ . For this high field a well-defined anomaly in  $dM/dT$  suggestive of magnetic ordering appears at  $\sim 90 \text{ K}$  (inset). In parallel, as seen in Fig. 1b the isothermal  $MH$  curves become S-shaped below  $\sim 90 \text{ K}$ . This shape is definitely different from the convex and soon saturated type of  $\text{BaFeO}_3$ ,<sup>10,11</sup> indicating that the GHM-FM transition for  $x=0.2$  proceeds more gradually over a wide field range than the AHM-FM transition for  $x=0$  but is (almost) completed at  $H = 50 \text{ kOe}$ .

The large difference in the temperature of rapidly changing  $M$  between  $H = 1 \text{ kOe}$  ( $50 \text{ K}$ ) and  $50 \text{ kOe}$  ( $90 \text{ K}$ ) should not be taken as indicating that the magnetic ordering temperature is strongly  $H$ -dependent. Mössbauer spectroscopic measurements in the absence of external field have revealed that the GHM-type ordering sets in at  $\sim 90 \text{ K}$  as will be reported elsewhere. The sharp change of  $M$  at  $\sim 50 \text{ K}$  for  $H = 1 \text{ kOe}$  should rather be assigned to the field-induced generation of FM domains in the GHM matrix. To get additional information, we have constructed the Arrott plot ( $H/M$  vs.  $M^2$ ) at  $89 \text{ K}$ , which is shown in the inset to Fig. 1(b). According to the criterion proposed,<sup>22</sup> the slope of this plot is negative for a first order magnetic transition (FOMT), while it is positive for a second order magnetic transition (SOMT). The present result shows that the transition for  $x=0.2$  is a FOMT-type, while BFO is a SOMT-type.<sup>10</sup>

Ordinal FOMT systems show both thermal and magnetic hystereses.<sup>1</sup> Compared in Figure 1(c) are the  $MH$  curves for  $x=0$  and  $0.2$  at  $4.5 \text{ K}$ . The curve for  $x=0$  is reversible within experimental error<sup>10</sup> but the curve for  $x=0.2$  is hysteretic. The field-induced magnetization is saturated at  $\sim 15 \text{ kOe}$  for  $x=0$  but a high field of  $\sim 35 \text{ kOe}$  is needed for  $x=0.2$ . The remarkable inconsistency between the 1st and 2nd loops for  $x=0.2$  reflects complicated processes of the GHM-FM transition. However, the variation of saturation magnetization from  $3.5 \mu_{\text{B}}/\text{Fe}$  for  $x=0$  to  $3.2 \mu_{\text{B}}/\text{Fe}$  for  $x=0.2$  is small, indicating that the basic electronic structure of  $\text{Fe}^{3+}\underline{\text{L}}$  is preserved. This kind of hysteresis, which hinders efficient magnetic refrigeration, essentially disappears above  $\sim 50 \text{ K}$  fortunately. These results suggest that the MCE of BSFO at  $x = 0.2$  should be considerably different from that of pure BFO in various aspects, not only in lowering of the working temperature.

Figure 2(a) shows the change of magnetic entropy ( $\Delta S$ ) calculated from  $MH$  curves based on the Maxwell equation:<sup>23,24</sup>

$$\Delta S = \int_0^H (\partial M / \partial T)_H dH = (1/\Delta T) \left( \int_0^H M(T + \Delta T) dH - \int_0^H M(T) dH \right). \quad (1)$$

Here,  $\Delta T$  stands for an increment in measuring temperature. It is well known that a problem may arise for FOMT systems because  $\partial M / \partial T$  becomes infinite at the  $T_C$ , leading to a spike-like artifact of  $\Delta S$ .<sup>1</sup> However, this problem does not apply to the present system showing mild field-dependences.<sup>1,25</sup> Moreover, note that the  $MH$  curves were measured in the loop process to avoid observing the artifact; each measurement was performed after resetting the sample by heating up to a temperature well above  $T_C$  (nearly room temperature).<sup>20</sup> Also,  $MH$  curves for FOMT should be averaged over the processes of increasing and decreasing field<sup>25</sup> because any artifact caused by hysteresis can be eliminated. However, from Fig. 2(a) as well as 1(b), such a correction is unnecessary in the temperature range of interest,  $T_1 \leq T \leq T_2$ . Here,  $T_1$  and  $T_2$  are the temperatures where the value of  $-\Delta S$  is decreased to 50% of the maximum.

The  $T$ - and  $H$ -dependence of  $-\Delta S$  for  $x=0.2$  is plotted in Fig. 2(a). At every fixed  $H$ ,  $-\Delta S$  shows a peak at a certain temperature,  $T(-\Delta S_{\max})$ , which becomes higher with increasing  $H$ . This tendency is similar to that of the temperature where  $dM/dT$  shows a negative peak,  $T((dM/dT)_{\min})$ , indicating that the entropy change is due to the field-induced change of magnetism. The peak value of  $-\Delta S_{\max} = \sim 4.9 \text{ J kg}^{-1} \text{ K}^{-1}$  for  $H = 50 \text{ kOe}$  is considerably smaller than that of BFO ( $\sim 5.8 \text{ J kg}^{-1} \text{ K}^{-1}$  at  $T(-\Delta S_{\max}) \sim 116 \text{ K}$ ).<sup>10</sup> The  $H$ - and  $T$ -dependence of  $-\Delta S$  is also different. Firstly, the  $H$ -dependence of  $T(-\Delta S_{\max})$  is much stronger: For BFO  $T(-\Delta S_{\max})$  increases only by  $\sim 4 \text{ K}$  as the field is increased from 10kOe to 50kOe,<sup>10</sup> while it is raised by  $\sim 20 \text{ K}$  for  $x=0.2$ . Secondly, the temperature dependence of  $-\Delta S$  for  $x=0.2$  is remarkably broadened below  $T(-\Delta S_{\max})$  though it is rather sharp for BFO. Thirdly,

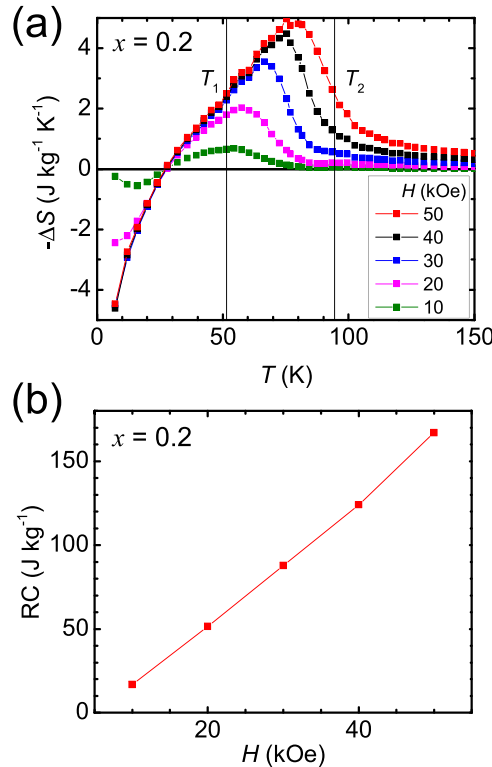


FIG. 2. (a) Magnetic entropy change ( $-\Delta S$ ) plotted against temperature ( $T$ ) for  $x=0.2$  with several  $H$  values ( $H$ : magnetic field).  $T_1$  and  $T_2$  are the temperatures of the cold and hot limit reservoirs for  $H=50 \text{ kOe}$  ( $T_1 \sim 51 \text{ K}$ ,  $T_2 \sim 94 \text{ K}$ ), respectively, which provide the refrigeration temperature range used for the calculation of refrigerant capacity ( $RC$ ; Fig. 2b). (b)  $RC$  values plotted against  $H$ , calculated from Fig. 2(a).

$T(-\Delta S_{\max}) \sim 77$  K for  $H=50$  kOe is lower than  $T((dM/dT)_{\min}) \sim 90$  K (Fig. 1), while it is opposite for BFO:  $T(-\Delta S_{\max}) \sim 116$  K is higher than the magnetic transition temperature of  $\sim 110$  K. These differences should have resulted from the difference in magnetism between GHM ( $x=0.2$ ) and AHM ( $x=0$ ). By the way, as seen in Figure 2(a)  $-\Delta S$  becomes negative below  $\sim 20$  K as observed for  $x=0$  too.<sup>10</sup> This is because  $\partial M/\partial T$  remains positive at relatively low fields due to the GHM state, as can be seen in Fig. 1(a).

The refrigerant capacity (RC), which is the thermal energy transferred in a single refrigeration cycle, can be evaluated by integrating  $-\Delta S$  over the refrigeration range of  $T_1 \sim T_2$ . Here,  $T_1$  and  $T_2$ , where  $|\Delta S| = 1/2|\Delta S_{\max}|$ , are considered to be the temperatures of the cold and hot limit reservoirs, respectively.<sup>7-10,19</sup> For  $H=50$  kOe,  $T_1 \sim 51$  K and  $T_2 \sim 94$  K and RC  $\sim 167$  J kg<sup>-1</sup>, which is very close to that of BFO,  $\sim 172$  J kg<sup>-1</sup>.<sup>10</sup> The refrigeration range ( $T_1-T_2$ ) of  $\sim 43$  K is also close to that of BFO ( $\sim 39$  K;  $T_1 \sim 103$  K,  $T_2 \sim 142$  K). The  $H$ -dependence of RC is plotted in Fig. 2(b). The similarity in RC between  $x=0$  and 0.2 is in accord with the general understanding that the RC mainly depends on saturation magnetization.<sup>26</sup>

The refrigeration temperature can be controlled between  $\sim 77$  K and  $\sim 116$  K by changing  $x$  between 0.2 and 0 as shown below. Figure 3(a) demonstrates the results for  $x=0.1$ , which is the borderline composition showing the AHM-FM transition.<sup>17</sup> For  $H = 50$  kOe,  $-\Delta S_{\max} \sim 5.8$  J kg<sup>-1</sup> K<sup>-1</sup> at  $\sim 98$  K (Fig. 3(a)) and RC  $\sim 160$  J kg<sup>-1</sup> with  $T_1 \sim 80$  K and  $T_2 \sim 116$  K (Fig. 3(b)). The performance was found to be both magnetically and thermally reversible, as seen for both  $x=0$  and  $x=0.2$ .

In comparison to Fe-doped MnV<sub>2</sub>O<sub>4</sub> (Mn<sub>1-x</sub>Fe<sub>x</sub>V<sub>2</sub>O<sub>4</sub> with  $x=0-0.3$ ),<sup>19</sup> its values of  $-\Delta S_{\max} \sim 5-6$  J kg<sup>-1</sup> K<sup>-1</sup> ( $H=40$  kOe, at  $\sim 77$  K) are larger by  $\sim 30\%$  than that of Ba<sub>0.8</sub>Sr<sub>0.2</sub>FeO<sub>3</sub>. From the viewpoint of application to magnetic refrigerators, however, the magnitude of  $-\Delta S_{\max}$  should better be expressed in the unit of per volume than in the unit of per weight, although the latter unit is widely used.<sup>1</sup> The density of the present system is  $\sim 6.28$  g/cm<sup>3</sup>, which is  $\sim 30\%$  greater than that of Mn<sub>1-x</sub>Fe<sub>x</sub>V<sub>2</sub>O<sub>4</sub> ( $\sim 4.75$  g/cm<sup>3</sup>; Mn<sub>0.7</sub>Fe<sub>0.3</sub>V<sub>2</sub>O<sub>4</sub>). Thus,  $-\Delta S_{\max}$  in the unit of per volume

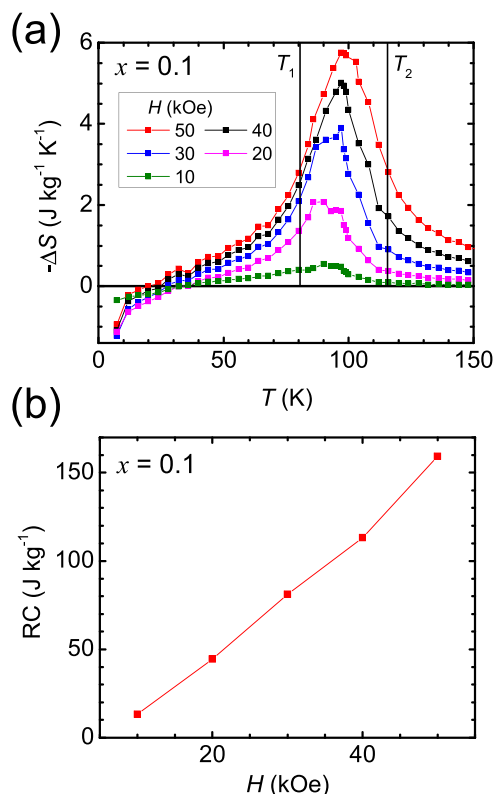


FIG. 3. (a) Magnetic entropy change ( $-\Delta S$ ) plotted against temperature ( $T$ ) for Ba<sub>0.9</sub>Sr<sub>0.1</sub>FeO<sub>3</sub> ( $x=0.1$ ) with several  $H$  values ( $H$ : magnetic field). (b) RC values plotted against  $H$ , calculated from Fig. 3(a).



is nearly the same for both systems. The peak temperature of  $-\Delta S_{\max}$  of  $\text{Mn}_{1-x}\text{Fe}_x\text{V}_2\text{O}_4$  is tuned between  $\sim 57$  and  $\sim 77$  K,<sup>19</sup> while that of  $\text{Ba}_{1-x}\text{Sr}_x\text{FeO}_3$  can be varied between  $\sim 77$  K and  $\sim 116$  K; as noted, the present system covers the temperature regions for natural gas and cuprates as well as for  $\text{N}_2$ . Since the presence or absence of magnetic hysteresis and also some parameters such as  $T_1$ - $T_2$  were not explicitly reported for  $\text{Mn}_{1-x}\text{Fe}_x\text{V}_2\text{O}_4$ , detailed comparison will be done in the future. Also, the other parameters such as the adiabatic temperature change ( $\Delta T_{\text{ad}}$ ) should be determined.

This work was partially supported by JSPS KAKENHI (25620071).

- <sup>1</sup> K. A. Gschneidner, Jr., V. K. Pecharsky, and A. O. Tsokol, *Rep. Prog. Phys.* **68**, 1479 (2005).
- <sup>2</sup> X. Moya, S. Kar-Narayan, and N. D. Mathur, *Nat. Mater.* **13**, 439 (2014).
- <sup>3</sup> V. K. Pecharsky and K. A. Gschneidner, Jr., *Phys. Rev. Lett.* **78**, 4494 (1997).
- <sup>4</sup> H. Wada and Y. Tanabe, *Appl. Phys. Lett.* **79**, 3302 (2001).
- <sup>5</sup> F.-X. Fu, B.-G. Shen, J.-R. Sun, Z.-H. Cheng, G.-H. Rao, and X.-X. Zhang, *Appl. Phys. Lett.* **78**, 3675 (2001).
- <sup>6</sup> A. Fujita, D. Matsunami, and H. Yako, *Appl. Phys. Lett.* **104**, 122410 (2014).
- <sup>7</sup> L. M. da Silva, A. O. dos Santos, A. A. Coelho, and L. P. Cardoso, *Appl. Phys. Lett.* **103**, 162413 (2013).
- <sup>8</sup> N. S. Bingham, M. H. Phan, H. Srikanth, M. A. Torija, and C. Leighton, *J. Appl. Phys.* **106**, 023909 (2009).
- <sup>9</sup> P. Lampen, N. S. Bingham, M. H. Phan, H. Kim, M. Osofsky, A. Piqué, T. L. Phan, S. C. Yu, and H. Srikanth, *Appl. Phys. Lett.* **102**, 062414 (2013).
- <sup>10</sup> M. Mizumaki, K. Yoshii, N. Hayashi, T. Saito, Y. Shimakawa, and M. Takano, *J. Appl. Phys.* **114**, 073901 (2013).
- <sup>11</sup> N. Hayashi, T. Yamamoto, H. Kageyama, M. Nishi, Y. Watanabe, T. Kawakami, Y. Matsushita, A. Fujimori, and M. Takano, *Angew. Chem. Int. Ed.* **43**, 12547 (2011).
- <sup>12</sup> E. Bocquet, A. Fujimori, T. Mizokawa, T. Saitoh, H. Namatame, S. Suga, N. Kimizuka, Y. Takeda, and M. Takano, *Phys. Rev. B* **45**, 1561 (1992); M. Abbate, F. M. F. de Groot, J. C. Fuggle, A. Fujimori, O. Strebel, F. Lopez, M. Domke, G. Kaindl, G. A. Sawatzky, M. Takano, Y. Takeda, H. Eisaki, and S. Uchida, *Phys. Rev. B* **46**, 4511 (1992).
- <sup>13</sup> M. Mizumaki, H. Fujii, K. Yoshii, N. Hayashi, T. Saito, Y. Shimakawa, T. Uozumi, M. Takano, *Phys. Stat. Sol. (c)* **12**, 818 (2015).
- <sup>14</sup> T. Lu and K. S. Wang, *Appl. Therm. Eng.* **29**, 1478 (2009).
- <sup>15</sup> S. Fujieda, A. Fujita, N. Kawamoto, and K. Fukamichi, *Appl. Phys. Lett.* **89**, 062504 (2006).
- <sup>16</sup> S. Ishiwata, M. Tokunaga, Y. Kaneko, D. Okuyama, Y. Tokunaga, S. Wakimoto, K. Kakurai, T. Arima, Y. Taguchi, and Y. Tokura, *Phys. Rev. B* **84**, 054427 (2011).
- <sup>17</sup> N. Hayashi, T. Yamamoto, A. Kitada, A. Matsuo, K. Kindo, J. Hester, H. Kageyama, and M. Takano, *J. Phys. Soc. Jpn.* **82**, 113702 (2013).
- <sup>18</sup> V. K. Pecharsky and K. A. Gschneidner, Jr., *J. Magn. Magn. Mater.* **200**, 44 (1999).
- <sup>19</sup> X. Luo, Y. P. Sun, L. Hu, B. S. Wang, W. J. Lu, X. B. Zhu, Z. R. Yang, and W. H. Song, *J. Phys.: Cond. Matter* **21**, 436010 (2009); Z. H. Huang, X. Luo, L. Hu, S. G. Tan, Y. Liu, B. Yuan, J. Chen, W. H. Song, and Y. P. Sun, *J. Appl. Phys.* **115**, 034903 (2014).
- <sup>20</sup> L. Caron, Z. Q. Ou, T. T. Nguyen, D. T. Cam Thanh, O. Tegus, and E. Brück, *J. Magn. Magn. Mater.* **321**, 3559 (2009); L. Caron, X. F. Miao, J. C. P. Klaasse, S. Gama, and E. Brück, *Appl. Phys. Lett.* **103**, 112404 (2013); L. von Moos, C. R. H. Bahl, K. K. Nielsen, and K. Engelbrecht, *J. Phys.:D* **48**, 025005 (2015).
- <sup>21</sup> M. Sato and Y. Ishii, *J. Appl. Phys.* **66**, 983 (1989).
- <sup>22</sup> S. K. Banerjee, *Phys. Lett.* **12**, 16 (1964).
- <sup>23</sup> V. Provenzano, A. J. Shapiro, and R. D. Shull, *Nature* **429**, 853 (2000).
- <sup>24</sup> V. K. Pecharsky and K. A. Gschneidner, *J. Appl. Phys.* **86**, 565 (1999).
- <sup>25</sup> J. S. Amaral and V. S. Amaral, *Appl. Phys. Lett.* **94**, 042506 (2009).
- <sup>26</sup> J. von Ranke, E. P. Nóbrega, I. G. de Oliveira, A. M. Gomes, and R. S. Sarthour, *Phys. Rev. B* **63**, 184406 (2001).